 CMES, vol.76, no.4, pp.217-233, 2011

Elastic Wave Propagation in Periodic Cellular Structures

B.Y. Tian[1], B. Tie[1], D. Aubry[1] and X.Y. Su[2]

Abstract: The present work is devoted to a theoretical analysis and numerical modeling of elastic wave propagation firstly in a one-dimensional periodic elastic rod structure and then in two-dimensional periodic elastic beam structures by using Bloch wave theorem. The dispersion relation between Bloch wave vectors and eigen frequencies is obtained and its dependency upon the micro-structural characteristics of the periodic cellular structure is analyzed. Thanks to the Bloch wave transforms, only the primitive cell is considered theoretically or numerically and the phenomena of frequency band-gaps and the diffracted waves caused by the periodic cells are modeled and analyzed.

Keywords: Periodic cellular structure, Bloch wave theorem, frequency band-gap, diffracted waves.

1 Introduction

Periodic cellular structures composed of topological isomorphic cells have been widely used to make lightweight but high strength composite materials. Many cellular shapes and connection methods have been developed for various engineering applications, as for example the sandwich panels with a thin-walled honeycomb-type core, which has a rigid-jointed in-plane two-dimensional hexagonal, square or triangular cellular micro structure. Therefore there is a growing interest in understanding the dynamic behaviors of those periodic structures under transient loadings, especially the wave propagation behaviors within each cell and crossing adjacent cells for the frequency ranges where the waves can interact with the cells.

Periodic cellular structures are discontinuous in geometry and in material properties. To model such a structure in the static or low frequency (LF) cases, homogenized models are generally used, by neglecting the micro-structural details and

[1] Laboratory MSSMat, Ecole Centrale Paris, CNRS (UMR 8579), France.
[2] LTCS and Department of Mechanics and Aerospace Engineering, College of Engineering, Peking University, China

using an equivalent constitutive law with continuous mechanical characteristics instead [Gibson and Ashby (1988); Burton and Noor (1997)]. The classical homogenized models usually offer an efficient and reliable solution to investigate the static or LF dynamic behaviors of the periodic structures. However our previous works show that for the flexural wave propagation in the periodic honeycomb-type thin layers in high frequency (HF) ranges, the homogenized models fail to give appropriate simulation results [Grédé (2006, 2009); Tie *et al.* (2009)]. Indeed, for the HF ranges, the involved wavelength is as short as or even shorter than the cell's characteristic lengths, so interactions between the waves and the cells become important and result in complex deformations of cellular walls, which cannot be taken into account by the classical homogenized models. To make more accurate simulation, Davini *et al.* proposed several improved methods to look for the equivalent mechanical characteristics of the homogenized models in dynamic cases [Davini *et al.* (2011)]. However, it is believed that more appropriate modeling should consider and integrate the effects of the microstructure of periodic structures.

It has been observed that special wave phenomena, such as frequency passing and stop bands, exist when elastic wave propagating in periodic cellular structures [Brillouin (1953)]. The existence of the frequency band-gap highlights the fact that a periodic cellular structure is anisotropic for the elastic waves propagating in it. This anisotropy is due to the impedance mismatch generated by periodic discontinuities in geometry or material properties within one cell or between adjacent cells and therefore is frequency dependent [Langley (1997); Ruzzene (2003); Gonella *et al.* (2008)]. As an important consequence, periodic cellular structures can be considered as frequency or spatial filters when giving different patterns or structure designs [Sigmund and Jensen (2003)]. Some recent studies are concentrated on exploring the frequency band-gaps and some others focus on testing the wave directional characteristics of periodic cellular structures of different types, by using the Bloch wave theorem [Srikantha Phani (2006); Spadoni (2009); Tee (2010); Jeong *et al.* (2004)]. Indeed, the Bloch wave theorem is widely employed in quantum mechanics, photonics crystal and mechanical system fields, benefit from which the domain to be analyzed and modeled can be reduced from the entire periodic cellular structure to a primitive cell [Atkins *et al.* (2005); Brillouin (1953); Mead (1973, 1996)]. Otherwise, the influence of imperfections on frequency band-gap and in-plane waves propagation has also been investigated [Martinsson *et al.* (2003)].

The present work is devoted to the theoretical analysis and numerical modeling of elastic wave propagation in one-dimensional (1D) rod and two-dimensional (2D) beam rectangular or hexagonal periodic cellular structures, by using Bloch wave theorem. The dispersion relation between Bloch wave vectors and eigen frequencies are obtained. Therefore, the frequency band-gap of each structure is obtained

and analyzed. For the studied 1D periodic structure, the dependency of the frequency band-gap on the mismatch of the characteristic acoustic impedances within a primitive cell is highlighted, for the studied 2D periodic structures, the influence of the double thickness of cellular walls oriented in one direction on the frequency band-gap is analyzed. Otherwise, the diffracted waves caused by the periodic cells are simulated numerically and amplification phenomena are observed.

The paper is organized as follows: The direct/inverse Bloch wave transforms are introduced in the section 2. The theoretical and numerical analyses of the elastic wave propagation in 1D periodic rod structure is summarized in the section 3 and the cases of 2D beam periodic structures are considered in the section 4. Finally the main conclusions are given in the section 5.

2 Bloch wave theorem

Consider a periodic cellular structure Ω of space dimension N, a primitive cell Q_0 and a set of basis vector $\{\mathbf{e}_i\}_{i=1,\ldots,N}$, called direct cell basis, are defined so that the entire structure Ω can be obtained by repeating the primitive cell along the direct cell basis. Dual to Q_0 and $\{\mathbf{e}_i\}_{i=1,\ldots,N}$, a reciprocal cell Q_0^*, called the first Brillouin zone [Brillouin (1953)], and a reciprocal cell basis $\{\mathrm{e}_j^*\}_{j=1,\ldots,N}$, are also defined, which satisfy the following relation:

$$\begin{aligned} &\mathrm{e}_i \cdot \mathrm{e}_j^* = \delta_{ij} \\ &vol(Q_0)vol(Q_0^*) = 1 \end{aligned} \tag{1}$$

where δ_{ij} is the Kronecker delta.

For any non-periodic function V($\mathbf{x}$) defined on Ω, the Bloch wave theorem states that, for each wave vector $\mathbf{k}$ restricted in the first Brillouin zone, the Bloch wave function or Bloch wave mode, $V^B(\mathbf{x}, \mathbf{k})$, of V($\mathbf{x}$) is a periodic function that has the same periodicity as the structure Ω:

$$V^B(\mathrm{x},\ \mathrm{k}) = \sum\nolimits_n V\left(\mathrm{x} + n_i\lambda_i\mathrm{e}_i\right) e^{i\mathrm{k}.(\mathrm{x}\ +\ n_i\lambda_i\mathrm{e}_i)},\ for\ \forall\ \mathrm{k} \in Q_0^* \tag{2}$$

The equation (2) defines in fact the direct Bloch wave transformation, while the inverse Bloch wave transformation states that V($\mathbf{x}$) can be reconstituted by integrating all the $V^B(\mathbf{x}, \mathbf{k})$ in the Q_0^*:

$$V\left(\mathrm{x}\right) = \frac{1}{vol(Q_0^*)} \int_{Q_0^*} V^B(\mathrm{x},\ \mathrm{k})\, e^{-i\mathrm{k}.\mathrm{x}}\, d\mathrm{k} \tag{3}$$

Therefore by virtue of the Bloch wave theorem, a non-periodic function in a periodic cellular structure can be decomposed into its Bloch wave functions having

the same periodicity as the periodic structure. In other word, the wave propagation phenomena through the whole structure can be understood by investigating the Bloch wave functions only in the primitive cell, so lots of efforts can be saved when doing analysis and simulation.

3 Elastic wave propagation in a 1D periodic elastic rod structure

The first periodic cellular structure considered herein is a 1D periodic structure made of elastic rods. Its primitive cell is composed by two rigid-jointed elastic rods respectively of length l_1 and l_2, therefore the period of the structure is $\lambda = l_1 + l_2$ (**Figure 1**).

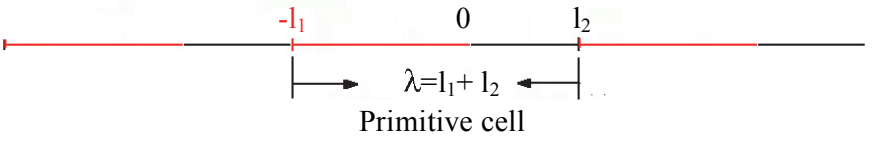

Figure 1: 1D elastic rod periodic structure

The equilibrium eigen equation of the i-th rod (i=1, 2) reads as:

$$\frac{d}{dx}\left[E_i \frac{dU(x)}{dx}\right] = -\rho_i \omega^2 U(x) \tag{4}$$

with (E_i, ρ_i) the Young's modulus and the density, $\omega\emptyset$ the eigen frequency and U(x) the corresponding eigen mode. By applying the direct Bloch wave transformation to the equation (4), the following Bloch eigen equation is obtained:

$$E_i \frac{\partial^2 U^B(x,\ k)}{\partial x^2} - 2ikE_i \frac{\partial U^B(x,\ k)}{\partial x} - E_i k^2 U^B(x,\ k) = -\rho_i \omega^2 U^B(x,\ k) \tag{5}$$

with $k \in Q_0^* = [0, 2\pi/\lambda[$ the Bloch wave vector and U^B(x, k) the Bloch wave mode of U(x). It is straightforward that the general solution of (5) has the following analytical form:

$$U_i^B(x,\ k) = a_i e^{i\left(k+\frac{\omega}{c_i}\right)x} + b_i e^{i\left(k-\frac{\omega}{c_i}\right)x} \tag{6}$$

where $c_i = \sqrt{E_i/\rho_i}$ is the wave velocity in the i-th rod. So solving (5) amounts to determining the four constants $(a_i, b_i)_{i=1,2}$.

Given a wave vector k, (ω, U^B(x, k)) are searched for the eigen problem (5) within the frequency range of interest and this solving results in the dispersion relation between k and ω.

3.1 Dispersion relation

Let us consider the primitive cell (**Figure 2**).

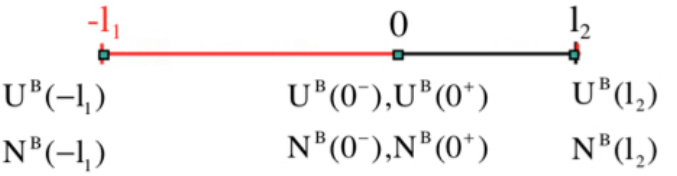

Figure 2: Interface conditions and periodic conditions

To calculate the constants $(a_i, b_i)_{(i=1,2)}$, the following interface conditions between the two rods at their junction point and periodic conditions at the ends of the primitive cell are considered:

$$\begin{aligned} &U^B(0^-) = U^B(0^+),\ N^B(0^-) = N^B(0^+) \\ &U^B(-l_1) = U^B(l_2),\ N^B(-l_1) = N^B(l_2) \end{aligned} \tag{7}$$

where N^B is the Bloch wave function of the axial force vector. Substituting the general solution form (6) into (7), we get the following system of four linear equations:

$$\begin{aligned} &U^B(0^-) = U^B(0^+),\ N^B(0^-) = N^B(0^+) \\ &U^B(-l_1) = U^B(l_2),\ N^B(-l_1) = N^B(l_2) \end{aligned} \tag{8}$$

with:

$$\begin{aligned} &U^B(0^-) = U^B(0^+),\ N^B(0^-) = N^B(0^+) \\ &U^B(-l_1) = U^B(l_2),\ N^B(-l_1) = N^B(l_2) \end{aligned}$$

To ensure that the system (8) admits nontrivial solutions (a_i, b_i), its determinant should vanish, which finally gives rise to a relation between k and ω, called dispersion relation. For the 1D rod structure, the dispersion equation can be put into the following simple analytical form:

$$\cos(\lambda k) = \cos(\omega T_1)\cos(\omega T_2) - \left(\frac{Z_1}{2Z_2} + \frac{Z_2}{2Z_1}\right)\sin(\omega T_1)\sin(\omega T_2) \tag{9}$$

where $Z_i = \rho_i c_i$ is the characteristic acoustic impedance of the i-th rod and $T_i = l_i/c_i$ the time for wave to pass through it. Based on the equation (9), for each given frequency ω, the Bloch wave vector $k = k_r + i\, k_{im}$ can be found and result in the following Bloch eigen mode in the i-th rod:

$$U_i^B(x,k) = a_i e^{i\left(k_r + \frac{\omega}{c_i}\right)x} e^{-k_{im}x} + b_i e^{i\left(k_r - \frac{\omega}{c_i}\right)x} e^{-k_{im}x} \tag{10}$$

Therefore, when k is real (k_{im} = 0), the Bloch eigen mode U_i^B is a propagating mode: It is transmitted to the adjacent cells with the same amplitude and there is no energy losing when propagating through the periodic structure. Otherwise, when k is complex or pure imaginary ($k_{im} \neq 0$), U_i^B is an evanescent mode: It vanishes rapidly when propagating to the adjacent cells and the pure energy exchanging between periodic cells is equal to zero [Mead (1973)].

The frequency ranges that give real values of k is called passing band and the others stop band. **Figure 3** gives the frequency band-gap of the 1D periodic rod structure: The red curves plot the two real solutions of k and indicate the passing bands, while the blue curves plot the imaginary part k_{im} of the two complex solutions of k, $j\pi/\lambda + i\, k_{im}$, (j=0, 1) and so indicate the stop bands.

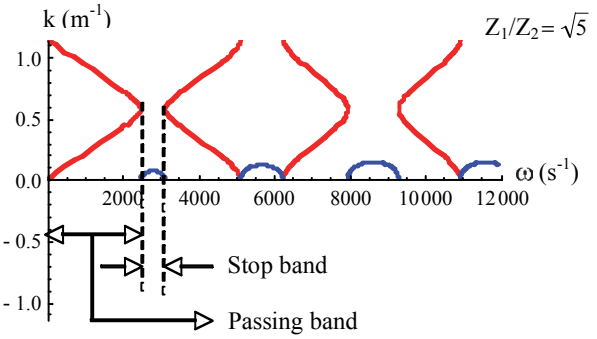

Figure 3: Frequency band-gap (Z_1/Z_2 = 1)

We remark that the location and the width of the stop bands strongly depend on the ratio between the two characteristic acoustic impedances Z_1/Z_2. The more the ratio is far from 1, the larger is the stop band and the stronger is the attenuation (**Figure 4**).

For the special case where Z_1/Z_2 = 1, according to the equation (9), we get k = ω/c_{avg}, with $c_{avg} = (l_1 + l_2)/(T_1 + T_2)$ the average wave propagation velocity in the primitive cell. In this case, all Bloch eigen modes are propagating and there is no stop bands (**Figure 5**).

3.2 Diffracted wave analysis

Now, we consider an incident plane wave $u_0(x,\ t) = e^{i(k_0 x - \omega_0 t)}$, with the wave vector k_0 and the angular frequency ω_0, and investigate how it propagates through the 1D periodic structure and how it is perturbed by the periodic cells. To do this, the wave

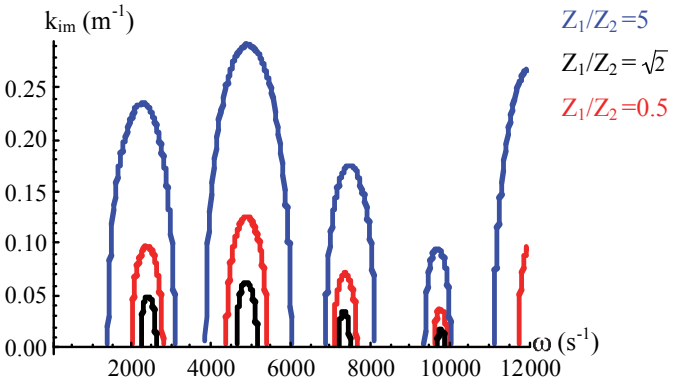

Figure 4: Influence of acoustic impedance ratio on the stop bands

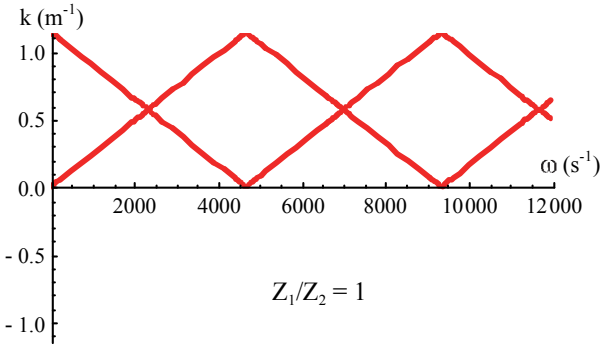

Figure 5: Frequency band-gap ($Z_1/Z_2 = 1$)

solution u(x, t) is decomposed into two parts in the following way:

$$u(x,\, t) = \left[e^{ik_0 x} + u_d(x)\right] e^{-i\omega_0 t} \tag{11}$$

We are interested in finding $u_d(x)$, the diffracted wave caused by the periodic cells, which indicate in fact the difference between the wave motion in a periodic structure and in a homogenous one. By substituting the equation (11) in the equilibrium eigen equation (4), we get:

$$\frac{d}{dx}\left[E_i \frac{du_d(x)}{dx}\right] + \underbrace{\left\{\frac{d}{dx}\left[E_i \frac{du_0(x)}{dx}\right] + \rho_i \omega_0^2 u_0(x)\right\}}_{f_e} = -\rho_i \omega_0^2 u_d(x) \tag{12}$$

where the second term of the left member is considered as an external loading f_e due to the incident wave. By expanding $u_d(x)$ as a linear combination of eigen mode U(x):

$$u_d(x) = \sum_n \alpha_n U_n(x) \tag{13}$$

Using the Bloch wave transform, for each k, the Bloch diffracted wave mode u_d^B can be then expressed as a linear combination of the Bloch eigen modes $U_n^B(x,\ k)$, already calculated:

$$u_d^B(x,\ k) = \sum_n \alpha_n(k) U_n^B(x,\ k) \tag{14}$$

So the aim now is to calculate the coefficient α_n(k).

Substituting the equation (14) into the Bloch transform of the equilibrium equation (12), we finally get:

$$\sum_n \rho_i(\omega^2 - \omega_0^2)\alpha_n(k) U_n^B(x,\ k) = f_e^B(x,\ k) \tag{15}$$

where f_e^B is the Bloch transform of the external loading, also expanded in terms of the Bloch eigen modes $U_n^B(x,\ k)$:

$$f_e^B(x,\ k) = \sum_n F_n(k) U_n^B(x,\ k) \tag{16}$$

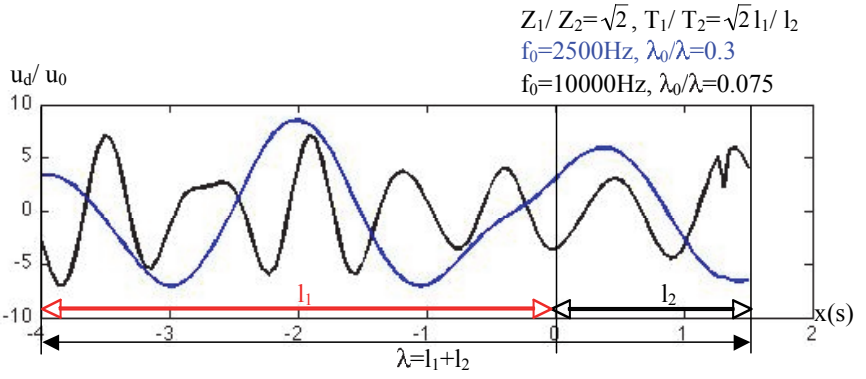

Figure 6: Wave amplification inside the primitive cell

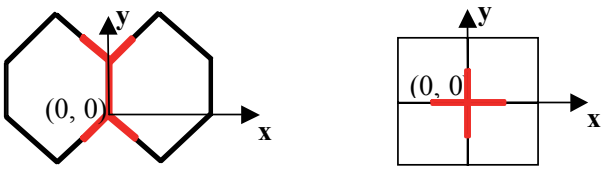

Hexagonal type cell (a) Rectangular type cell (b)

Figure 7: 2D elastic beam periodic cellular structures

Therefore α_n(k) can be obtained in the following way:

$$\alpha_n(k) = \frac{F_n(k)}{\rho_i(\omega^2 - \omega_0^2)} \tag{17}$$

Finally, the diffracted wave solution u_d is obtained by combining the equations (14) and (17), then by means of the inverse Bloch wave transformation.

In the present study, two incident waves with respectively two different frequencies f_0= 2.5kHz and f_0 = 10kHz are considered. For these two incident waves, the involved wavelength in the first rod, λ_0, is respectively 0.3 and 0.075 times of the primitive cell's size. **Figure 6** presents the ratio of amplitude between the incident wave u_0 and the diffracted wave u_d for the both cases. We observe firstly an important amplification phenomenon of wave amplitude due to the diffraction caused by the periodic cellular structure. Secondly, we remark that the amplification level seems not be significantly affected by the incident wave's frequency f_0.

4 Elastic wave propagation in 2D periodic elastic beam structures

In this section, we consider 2D elastic beam periodic structures with respectively hexagonal or rectangular cells (**Figure 7**).

4.1 Periodic hexagonal cellular structure

The primitive cell of periodic hexagonal cellular structure is composed of five rigid-jointed elastic beams (**Figure 7**(a), **Figure 8**). The Lamé coefficients and the density of all the beams are (λ, μ) and ρ, but the length s of the vertical beam B1 is twice the length of the other four beams. The thickness of the beam B1 is H_1 and of the others is H_0. Each beam is parameterized in its local coordinate system (**s**, **n**), where the axis **s** is parallel to the beam and the axis **n** is perpendicular to the beam

while the entire structure is considered in the global Cartesian coordinate system (**x**, **y**) (**Figure 8**).

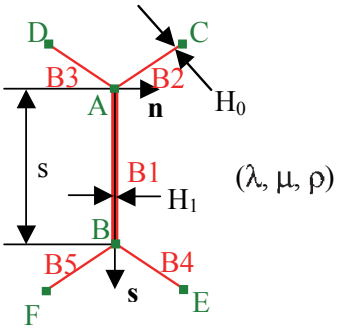

Figure 8: Primitive cell of the hexagonal structure

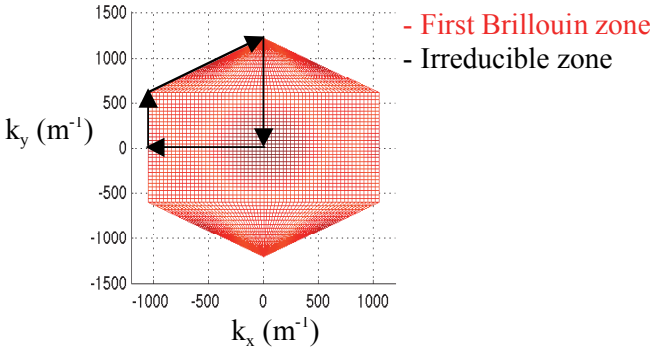

Figure 9: The first Brillouin zone and the irreducible zone of the hexagonal structure

The well-known Timoshenko kinematics for thick beams is used, so the displacement **u**(s, t) in each beam reads as:

$$\mathrm{u}(s,\ t) = u_{01}(s)\mathrm{s} + u_{02}(s)\mathrm{n} + t\ u_{13}(s)\mathrm{s} \tag{18}$$

where u_{01}(s) and u_{02}(s) are the displacement of the middle line in direction **s** and **n**, u_{13}(s) the rotation of the fibers and t the thickness variable. For each beam, the

Bloch equilibrium eigen equations read as:

$$\begin{aligned}
&\frac{d^2U_{01}^B}{ds^2} - 2i(k,s)\frac{dU_{01}^B}{ds} - (k,s)^2U_{01}^B = -\frac{\rho\omega^2}{\lambda+2\mu}U_{01}^B \\
&\frac{d^2U_{02}^B}{ds^2} - 2i(k,s)\frac{dU_{02}^B}{ds} - (k,s)^2U_{02}^B + \frac{dU_{13}^B}{ds} = -\frac{\rho\omega^2}{\mu}U_{02}^B, \quad (m=0,1) \\
&\frac{d^2U_{13}^B}{ds^2} - 2i(k,s)\frac{dU_{13}^B}{ds} - \left[(k,s)^2 + \frac{12\mu}{(\lambda+2\mu)H_m^2}\right]U_{13}^B - \frac{12\mu}{(\lambda+2\mu)H_m^2}\frac{dU_{02}^B}{ds} \\
&= -\frac{\rho\omega^2}{\lambda+2\mu}U_{13}^B
\end{aligned} \tag{19}$$

For this periodic structure, the first Brillouin zone Q_0^* is a hexagonal cell. Similar to the analysis we did for the 1D periodic rod structure, giving k, we look for the eigen frequencies ω and the corresponding Bloch eigen modes (U_{01}^B, U_{02}^B, U_{13}^B) of (19).

To get the dispersion equation, we write the interface conditions between the five beams at the interior junction points and the following periodic conditions at the ends of the primitive cell (**Figure 8**). For example, at the point A, we write the continuity of the displacement and the equilibrium of the generalized beam forces and moments:

$$\begin{aligned}
&Y_{01}^{B(1)} + U_{02}^{B(1)} = U_{01}^{B(2)} + U_{02}^{B(2)} = U_{01}^{B(3)} + U_{02}^{B(3)} \\
&U_{13}^{B(1)} = U_{13}^{B(2)} = U_{13}^{B(3)} \\
&N^{B(1)} + Q^{B(1)} + N^{B(2)} + Q^{B(2)} + N^{B(3)} + Q^{B(3)} = 0 \\
&M^{B(1)} = M^{B(2)} = M^{B(3)}
\end{aligned} \tag{20}$$

where $\mathbf{N}^B$ is the Bloch axial force vector, $\mathbf{Q}^B$ is the Bloch transverse shear force vector and $\mathbf{M}^B$ is the Bloch bending moment. Similar junction conditions are also written at the point B. As for the periodic conditions, they consist also in the continuity of the displacement et the equilibrium of the generalized beam forces. For example, for the couple of points C and F, we have:

$$\begin{aligned}
&Y_{01}^{B(2)} + U_{02}^{B(2)} = U_{01}^{B(5)} + U_{02}^{B(5)} \\
&U_{13}^{B(2)} = U_{13}^{B(5)} \\
&N^{B(2)} + Q^{B(2)} + N^{B(5)} + Q^{B(5)} = 0 \\
&M^{B(2)} = M^{B(5)}
\end{aligned} \tag{21}$$

Similar periodic conditions should also be written for the couple of points D and E. Hence, we get an eigen problem of 30 equations to be solved.

Unfortunately, for the 2D studies, it is not possible to express the dispersion equation in an explicit analytical form as in the 1D case. Therefore we can only solve numerically (19) and plot the dispersion surfaces. One interesting way to simplify the numerical calculation and to observe more easily the frequency band-gap consists in looking for the eigen frequencies and the Bloch eigen modes only for those **k** locating on the contour of the irreducible zone instead of the whole first Brillouin zone (**Figure 9**) [Kittel (1962)].

Due to the manufactory process of periodic hexagonal cellular structure materials, usually the vertical beam B1 of the primitive cell has double thickness when compared with the other beams. Therefore, two cases are considered in this study: The first one with $H_1 = H_0$ and the second one with $H_1 = 2H_0$. The beam's slenderness of both cases is taken so that we have $2\sqrt{3}s/H_0 \approx 50$.

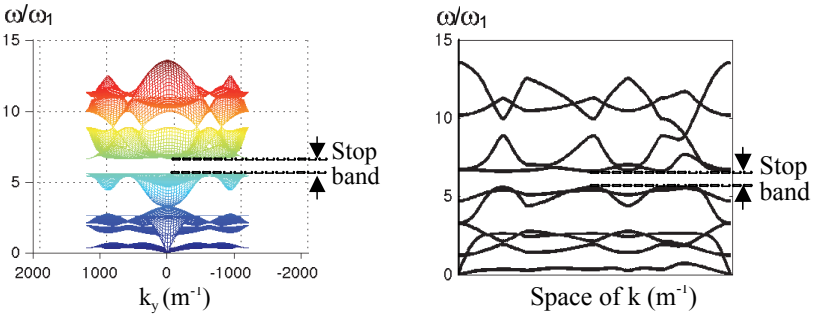

Figure 10: Dispersion surface and dispersion curve, $H_1 = H_0$

In the first case with $H_1 = H_0$, we find out that the first frequency stop band of the hexagonal cellular structure appears at the frequency that is about 5 times of the first pinned-pinned flexural resonance frequency of the beam, $\omega_1 = \pi^2\sqrt{EI/\rho H_0 s^4}$, with $I = 12/H_0^3$ (**Figure 10**). However, for the same frequency range, no obvious stop band is observed in the second case, as the first stop band seems to move to the higher frequency range (**Figure 11**).

4.2 Periodic rectangular cellular structure

The primitive cell of periodic rectangular cellular structure is composed of four rigid-jointed elastic beams with the same length s (**Figure 7**(b), **Figure 12**). The Lamé coefficients and the density of the beams are (λ, μ) and ρ. Denote the thickness of the beams B1 and B2 by H_1 and the one of the beams B3 and B4 by H_0.

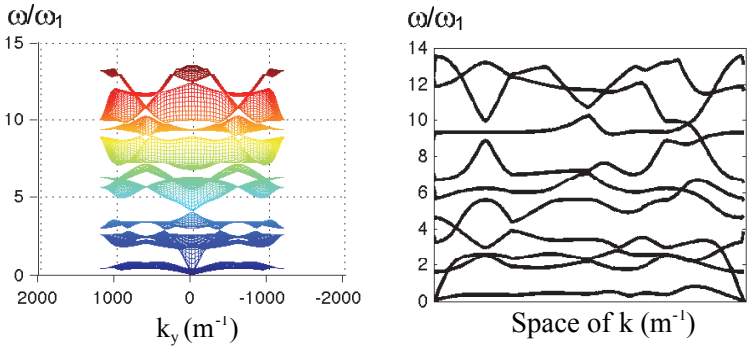

Figure 11: Dispersion surface and dispersion curve, $H_1 = 2H_0$

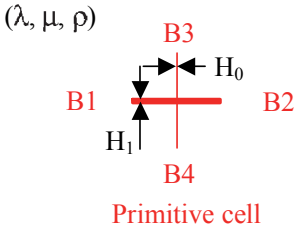

Figure 12: Primitive cell the periodic rectangular cellular structure

The Bloch equilibrium eigen equations are always given by (19). In this case, the first Brillouin zone is a rectangular cell (**Figure 13**). For all the Bloch wave vectors **k** included in the reciprocal cell, the corresponding eigen frequencies and Bloch eigen modes are calculated.

By writing the interface conditions and the periodic conditions, we get an eigen system composed of 24 equations, which can only be solved numerically. As in the previous case, two kinds of primitive cells are considered: $H_1 = H_0$ and $H_1 = 2H_0$. **Figure 14** and **Figure 15** show the plots of the dispersion surfaces and of the dispersion curves. As an important result, we remark that for the both rectangular cellular structures, no frequency band-gap exists in the whole frequency domain.

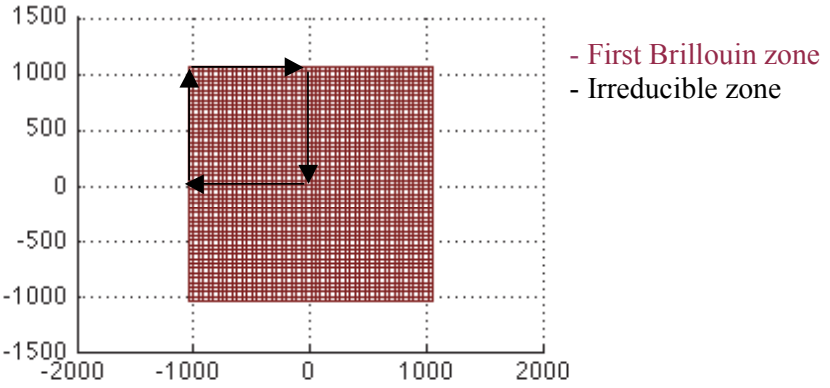

Figure 13: The first Brillouin zone and irreducible zone of the rectangular structure

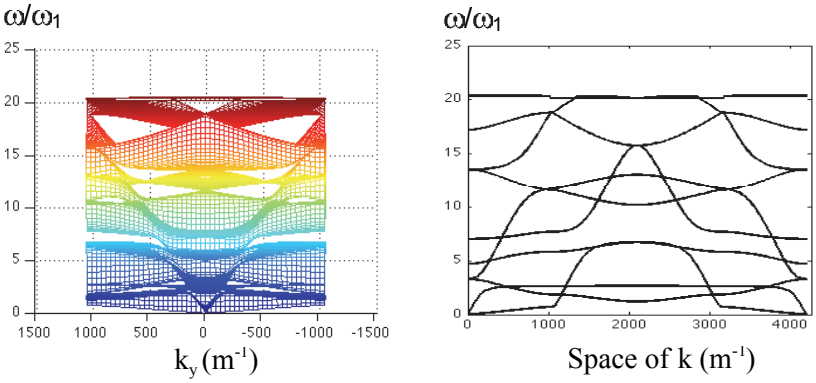

Figure 14: Dispersion surface and dispersion curve, $H_1 = H_0$

5 Conclusions

Our previous work shows that the classical homogenized models fail to correctly describe the HF flexural wave propagation phenomena of the periodic hexagonal cellular structures. To get appropriate modeling, we cannot neglect no more the effects coming from the interaction between the HF waves and the periodic microstructure. Hence, in this work, we propose to take the advantage of the Bloch wave theorem, which allows to take into account the geometric and mechanical characteristics of the cells, in order to optimize numerical models and save compu-

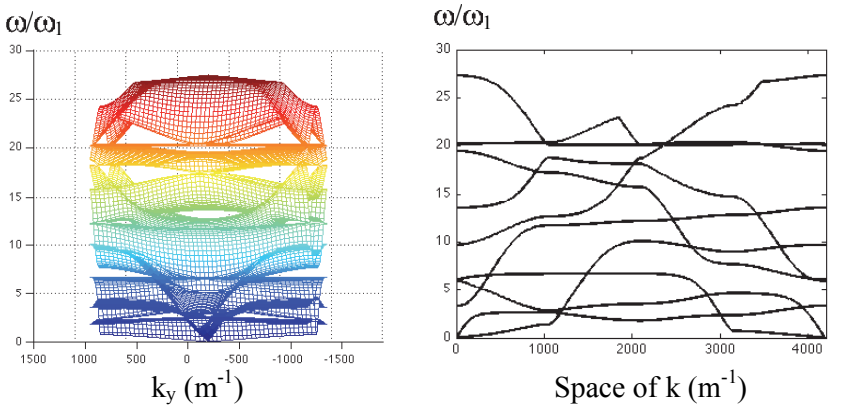

Figure 15: Dispersion surface and dispersion curve, $H_1 = 2H_0$

tational costs.

Theoretical analyzing and FE numerical modeling tools based on the Bloch wave theorem are developed and validated. They are at first applied to a 1D periodic structure composed of elastic rods. By considering the sole primitive cell, the dispersion relation is obtained analytically and numerically, and the frequency passing and stop bands calculated. The dependency of the frequency band-gap upon the ratio between the different characteristic acoustic impedances is analyzed. When an incident plane wave is injected in the periodic structure, diffracted waves are triggered by the periodically placed cells and wave amplitudes are amplified. Our numerical analyses show that this amplification phenomenon is independent on the incident wave frequency.

Our methods are also applied to the 2D periodic hexagonal and rectangular cellular structures composed by elastic beams. The frequency band-gaps are evaluated numerically and dispersion surfaces and curves are plotted. The influence of the beam's thickness on the frequency band-gap is considered. For the hexagonal cellular structure it is found out that the double thickness of the vertical beams makes the first stop band move to HF range. In the case of the rectangular cellular structure, no frequency stop band exists.

References

Atkins, P.; Friedman, R. (2005): *Molecular quantum mechanics.* Oxford University Press.

Brillouin, L. (1953): *Wave propagation in the periodic structures.* Dover Publication.

Burton, W. S.; Noor, A. K. (1997): Assessment of continuum models for sandwich panel honeycomb cores. *Computational Methods in Applied Mechanics and Engineering*, vol. 145, pp. 341–360.

Davini, C.; Ongaro, F. (2011): A homogenized model for honeycomb cellular materials. *J. Elast.*, vol. 104, pp. 205–226.

Gibson, L. J.; Ashby, M. F. (1988): *Cellular solids: Structures and properties.* International Series on Material Science & Technology. Pergamon Press.

Gonella, S.; Ruzzene, M. (2008): Analysis of in-plane wave propagation in hexagonal and re-entrant lattices. *J. Sound Vib.*, vol. 312, pp. 125–139.

Grédé, A.; Tie, B.; Aubry, D. (2006): Elastic wave propagation in hexagonal honeycomb sandwich panels: Physical understanding and numerical modeling. *Journal de Physique*, vol. 134, pp. 507–514.

Grédé, A (2009): *Modélisation des chocs d'origine pyrotechnique dans les structures d'Ariane5: dévéloppement de modèles de propagation et d'outils de modélisation*. PhD Thesis.

Jeong, S. M.; Ruzzene, M. (2004): Analysis of vibration and wave propagation in cylindrical grid-like structures. *Shock and Vibration*, vol. 11, pp. 311–331.

Kittel, C. (1962): *Elementary solid state physics: A short course.* 1^{st} ed., Wiley.

Langley, R. S.; Bardell, N. S.; Ruivo, H. M. (1997): The response of two-dimensional periodic structures to harmonic point loading: a theoretical and experimental study og a beam grillage. *J. Sound Vib.*, vol. 207, pp. 521–535.

Martinsson, P. G.; Movchan, A. B. (2003): Vibrations of lattice structures and phononic bandgaps. *The Quarterly Journal of Mechanics and Applied Mathematics*, vol. 56, pp. 45–64.

Mead, D. J. (1973): A general theory of harmonic wave propagation in linear periodic systems with multiply coupling. *J. Sound Vib.*, vol. 27, pp. 235–260.

Mead, D. J. (1996): Wave propagation in continuous periodic structures: research contributions from Southampton 1964-1995. *J. Sound Vib.*, vol. 190, pp. 495–524.

Ruzzene, M.; Scarpa, F.; Soranna, F. (2003): Wave beaming effects in two-dimensional cellular structures. *Smart Mater. Struct.*, vol. 12, pp. 363–372.

Sigmund, O.; Jensen, J. S. (2003): Systematic design of photonic band-gap materials and structures by topology optimization. *Philosophical Transactions of the Royal Society London Series A (Mathematical, Physical and Engineering Sciences)*, vol. 361, pp. 1001–1019.

Spadoni, A.; Ruzzene, M.; Gonella, S.; Scarpa, F. (2009): Phononic properties of hexagonal chiral lattices. *Wave motion*, vol. 46, pp. 435–450.

Srikantha Phani, A.; Woodhouse, J.; Fleck, N. A. (2006): Wave propagation in two-dimensional periodic lattices. *J. Acoust. Soc. Am.*, vol. 119, no. 4, pp. 1995–2005.

Tee, A.; Spadoni, A.; Scarpa, F.; Ruzzene, M. (2010): Wave propagation in auxetic tetrachiral honeycombs. *Journal of Vibration and Acoustics*, vol. 132, pp. 031007-1–031007-8.

Tie, B.; Aubry, D.; Grédé, A.; Philippon, J.; Tian, B.; Roux, P. (2009): Predictive Numerical Modeling of Pyroshock Propagation in Payload Adaptors of Space launcher. *11th ECSSMMT European Conference on Spacecraft Structures, Materials & Mechanical Testing (CNES ESA DLR)*, September 15-17, 2009, Toulouse, France.

Zhou, J.T. and Q.W. Ma, Q.W.(2010): MLPG Method Based on Rankine Source Solution for Modelling 3D Breaking Waves *CMES: Computer Modeling in Engineering and Science*, vol.56, no.2, pp.179-210.